MEASUREMENTS OF CHARMED PARTICLES LIFETIMES

L. Foà

Istituto di Fisica, Università di Pisa
INFN - Sezione di Pisa
Italy

All experiments aiming to measure the lifetime of charmed particles consist of two separate parts : an high resolution vertex detector for measuring the length of the decay path of individual particles and a forward spectrometer for identifying the events and for measuring the energy of the secondaries of the decay. All spectrometers have been designed to handle many prong events, to detect γ-rays and to identify charged and neutral kaons.

In general the vertex detectors make use of visual techniques and consist of nuclear emulsions or bubble chambers with improved space resolution ($\sigma < 50$ μm). One of the experiments described below, on the contrary, makes use of solid state detectors to measure the lifetime of charged mesons in a purely electronic way.

A variety of beams have been used to produce the charmed pairs (neutrinos, photons, pions and protons) coupled to various vertex detectors. Table 1 shows a list of the experiments performed in the last years and presented to the Lisbon Conference or to this Symposium.

TABLE 1

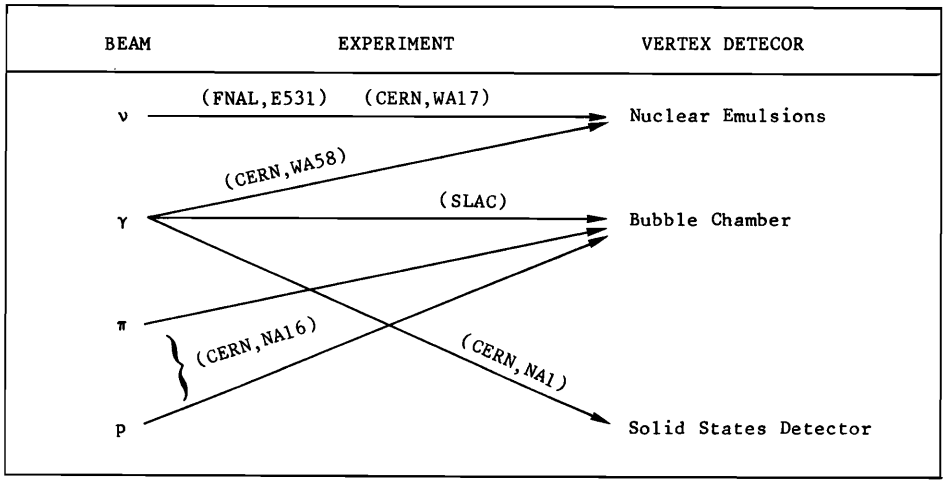

Two of the experiments which have contributed to this Conference are based on the use of bubble chambers. In the first one [1], NA 16, an hadronic beam of 360 GeV/c is sent into a small LEXAN bubble chamber (LEBC, 20 cm in diameter and 4 cm deep) which provides a resolution of

∿ 35 μm. Secondaries of charmed particle decays are detected by the European Hybrid Spectrometer shown in Fig. 1, which consists of a two-stage momentum analysis (magnets 1 and 2), proportional and drift chambers, an intermediate and a forward gamma detectors. A limited information on the nature of the detected particles is provided by ISIS 1 which measures the dE/dx of each secondary particle on a sample of 50 wires.

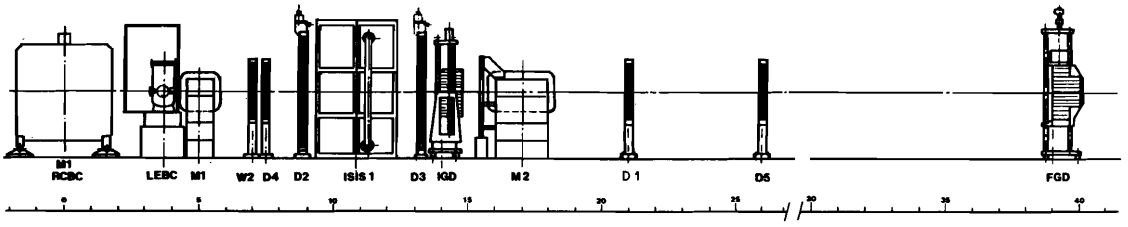

Fig. 1.- General lay-out of the EHS Spectrometer at the CERN SPS.

Up to now 300.000 pictures have been scanned looking for secondary vertices which could not be interpreted as strange particle decays. With reference to Fig. 2, a few conditions were set on the minimum decay length ℓ or on the minimum value of the impact parameter y_{max}, where "max" refers to the particle which has the maximum y in the decay. D^0's were accepted only if $\ell > 1$ mm allowing for a clear separation between interaction and decay vertices, while the identification of $D^{\pm}$ required the value of y_{max} to exceed 0.1 mm in order to avoid overlap of secondary and primary tracks.

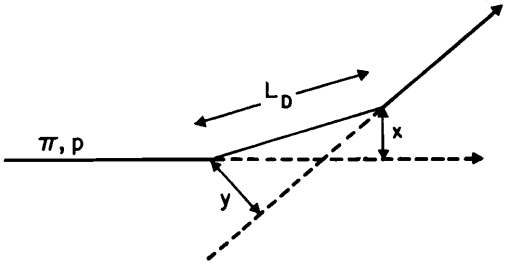

Fig. 2.- Definition of the kinematical variables used in the search of secondary vertices.

Only events fully recontructed in the spectrometer have been considered for the lifetime measurements. The best fit values for the average lifetimes have been evaluated by means of the expression

$$\frac{c\,\langle\tau\rangle}{m} = \frac{1}{N}\sum_{i=1}^{N}\frac{\ell_i - \ell_i^{min}}{P_i}$$

where ℓ_i is the decay path, ℓ_i^{min} is the minimum detectable path, p_i is the momentum of the D-meson and N is the number of events.

Tables 2 and 3 show the events used for the determination of τ_{D^0} and $\tau_{D^{\pm}}$.

TABLE 2

$D^{\pm}$ DECAYS

No.	CHANNEL	MASS(MEV)	$\tau(10^{-13}$ s)	BEAM
1	$D^- \to K^+\pi^-\pi^-$	1867 ± 7	8.05 ± 0.09	π
2	$D^- \to K^+\pi^-\pi^-\pi^0\pi^0$	1863 ± 20	12.7 ± 0.2	π
3	$D^+ \to K^-\pi^+\pi^+\pi^0$	1867 ± ∿ 100	13.9 ± 0.75	π
4	$D^- \to K^+\pi^-\pi^-$	1840 ± 12	0.84 ± 0.03	π
5	$D^+ \to K^-\pi^+\pi^+\pi^0$	1861 ± 12	11.8 ± 0.15	p
6	$D^- \to \pi^+\pi^-\pi^-\pi^0$	1861 ± 19	2.08 ± 0.03	p
7	$D^- \to K^+\pi^-\pi^-$	1859 ± 7	16.17 ± 0.18	p

TABLE 3

D^0 DECAYS

No	CHANNEL	MASS(MEV)	$\tau(10^{-13}$ s)	BEAM
1	$D^0 \to K^-\pi^+\pi^0\pi^0$	1857 ± 22	2.13 ± 0.06	π
2	$\bar{D}^0 \to K^+\pi^+\pi^-\pi^-$	1862 ± 9	5.92 ± 0.1	π
3	$\bar{D}^0 \to K^+\pi^-\pi^0\pi^0$	1820 ± 40	0.24 ± 0.02	π
4	$D^0 \to K^-\pi^+\pi^0\pi^0$	1880 ± ∿ 60	2.63 ± 0.09	π
5	$\bar{D}^0 \to K^+\pi^+\pi^-\pi^-$	1850 ± 4	2.67 ± 0.08	π
6	$D^0 \to K^-\pi^+\pi^0\pi^0$	1847 ± 20	2.10 ± 0.14	π
7	$D^0 \to K^-\pi^+\pi^0\pi^0\pi^0$	1840 ± 30	11.14 ± 1.24	p
8	$D^0 \to K^-\pi^+\pi^0$	1856 ± 11	31.6 ± 0.36	π

It is interesting to notice how important the detection of π^0's is for reaching a sufficient statistics: 10 events out of 15 would have been lost without it.

Fig 3 a and b show the logarithmic plots of the lifetimes. The results are

$$\tau_{D^0} = (3.2\ ^{+2.2}_{-1.0}) \times 10^{-13}\ \text{s}$$

$$\tau_{D^\pm} = (8.0\ ^{+4.9}_{-2.4}) \times 10^{-13}\ \text{s}\ .$$

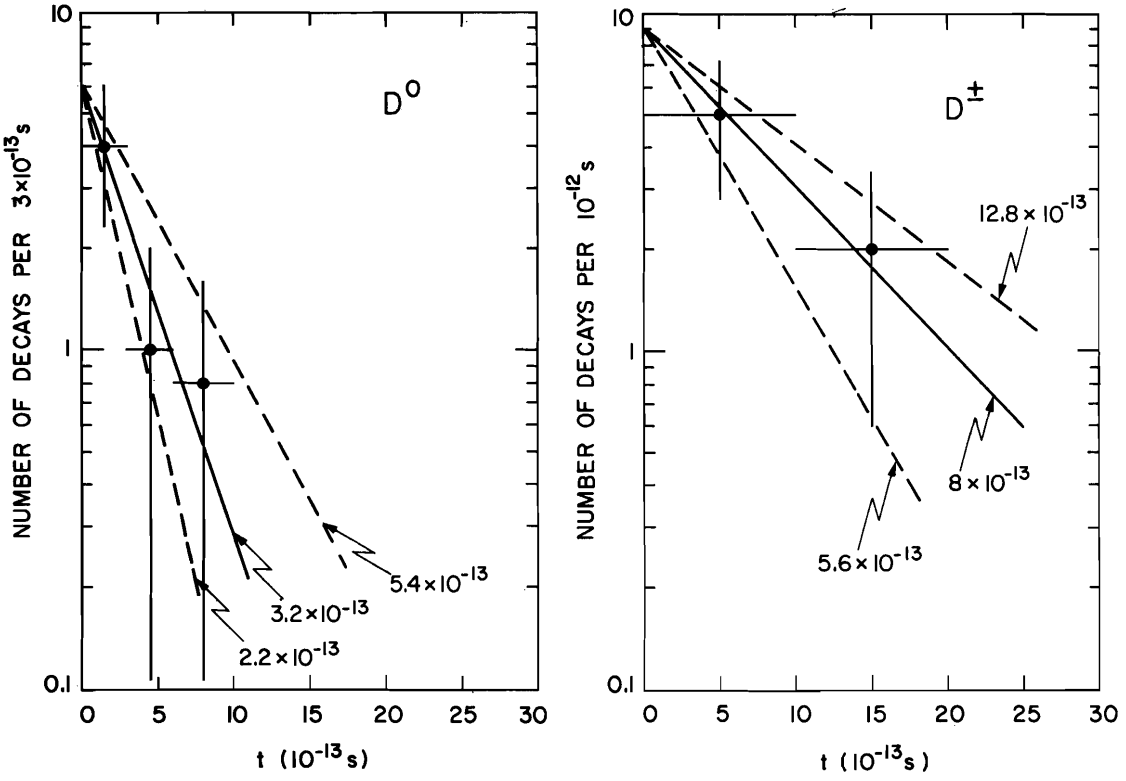

Fig. 3 Logarithmic plot of the lifetimes for neutral (a) and charged (b) D-mesons.

Data of similar quality have been presented by the SLAC Bubble Chamber Group [2]. A nearly monocromatic photon beam of 19.5 GeV (see Fig. 4) was produced by backscattering laser light on the SLAC electron beam and sent into the 40" bubble chamber.

This chamber was equipped with an additional high resolution camera which allowed a resolution of 55 μm over a depth of ± 6 mm. Downstream to the bubble chamber two multicell Cerenkov counters and a shower detector sketched in Fig. 5 identify hadronic events. A sample of 50.000 events has been analyzed searching for topologies typical of a charm decay. Fiducial regions are defined downstream to the interaction point, which are expected to contain 99% of D-meson decays. These "charm boxes" measure 0.5x5 mm² for D^0's and 1x10 mm² for $D^{\pm}$'s. Only 3,4,5 prong vertices or V's which failed to fit strange particle decays have been considered as candidates and used for the lifetime measurement subject to the condition that the impact parameter of at least one particle was larger than 130 μm. The final selection contains four $D^{\pm}$ decays, two events with a clear D^0 decay each and one event with two D^0 decays with an ambiguity in the attribution of a π^0.

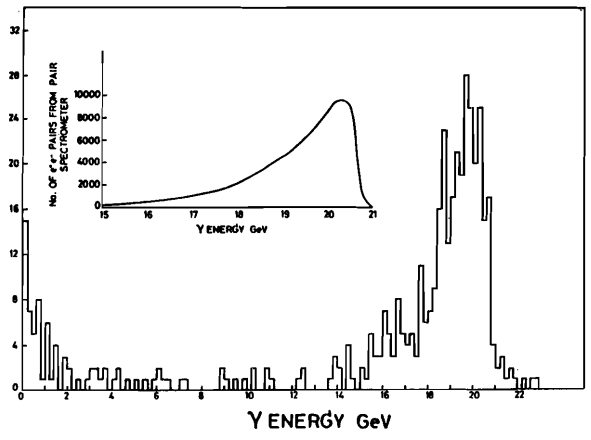

Fig. 4.- Energy spectrum of the SLAC photon beam.

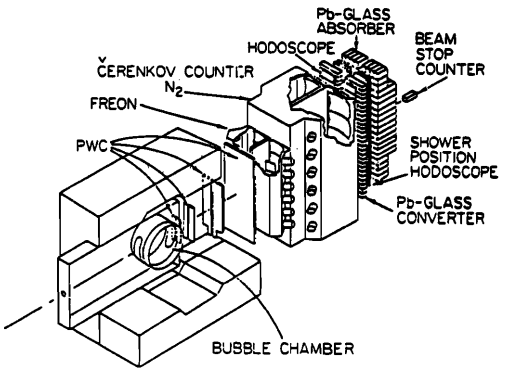

Fig. 5.- General lay-out of the 40" bubble chamber experiment.

The values of the lifetimes, determined by means of expression (1) are

$$\tau_{D^0} = (1.9^{+1.7}_{-0.6}) \times 10^{-13}\ s$$

$$\tau_{D^\pm} = (6.5^{+6.0}_{-2.1}) \times 10^{-13}\ s\ .$$

No new data have been presented at this conference by the groups working with nuclear emulsions. The results discussed at the Lisbon Conference are summarized, for comparison, on Table 4 [3].

TABLE 4

Experiment	FNAL (ν) Hyb. Em. Spectr.		CERN WA58 (γ) Emulsion-Ω		CERN WA17 (γ) Emulsion+BEBC	
	$\tau(10^{-13}\ s)$	Ev.	$\tau(10^{-13}\ s)$	Ev.	$\tau(10^{-13}\ s)$	Ev.
D^0	$3.0^{+1.1}_{-0.7}$	17	$1.34^{+1.2}_{-0.4}$	5	$0.5^{+0.6}_{-0.3}$	3
D^+	$9.5^{+6.5}_{-3.3}$	6				
F^+	$2.0^{+1.8}_{-0.8}$	3	4.4	8	$2.5^{+2.2}_{-1.1}$	5
Λ_c^+	$1.7^{+0.9}_{-0.5}$	6				

The third experiment consists of a purely electronic measurement of $D^{\pm}$ lifetime performed at CERN by the NA1 (FRAMM) Collaboration [4]. D-pairs are photoproduced coherently off silicon nuclei according to the diagram

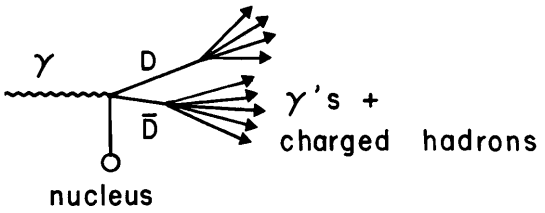

in the energy range $80 < E_\gamma < 150$ GeV. The choice of a coherent production mechanism has been made in order to transfer all the photon energy to the charmed mesons, with consequent large values of the relativistic γ-factors, and to limit the sample to a few almost exclusive channels ($D\bar{D}, D\bar{D}^* + D^*\bar{D}, D^*\bar{D}^*$) minimizing the combinatorial background.

A forward spectrometer (see Fig. 6), structured in four stages in order to provide an almost uniform momentum resolution between 1 and 150 GeV/c, reconstructs angle and momentum of charged particles. Two Cerenkov counters are installed inside the first two magnets to separate π's from K's between 4 and 20 GeV/c. A set of e.m. shower detectors with a hole at the centre are positioned in front of each magnet and at the end of the spectrometer to detect photons from π^0 decay.

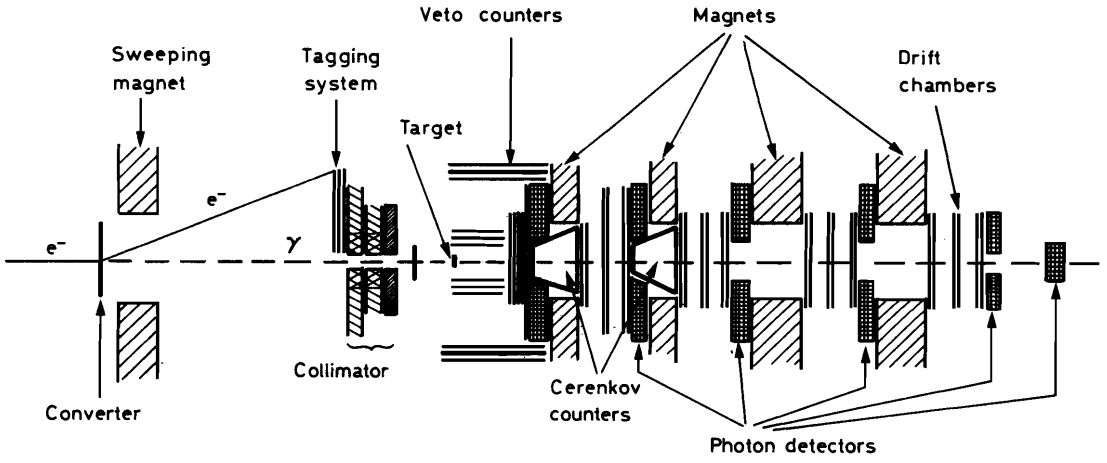

Fig. 6.- The NA1 (FRAMM) Spectrometer in the North Area of the CERN SPS.

The target consists of 40 layers of silicon detectors, each one 300 μm thick, spaced by 100 μm gaps. Altogether, the target is 1.6 cm thick, corresponding to 15% of a radiation length. The signal of each layer is proportional to the number of crossing minimum ionizing particles, as shown in Fig. 7 [5].

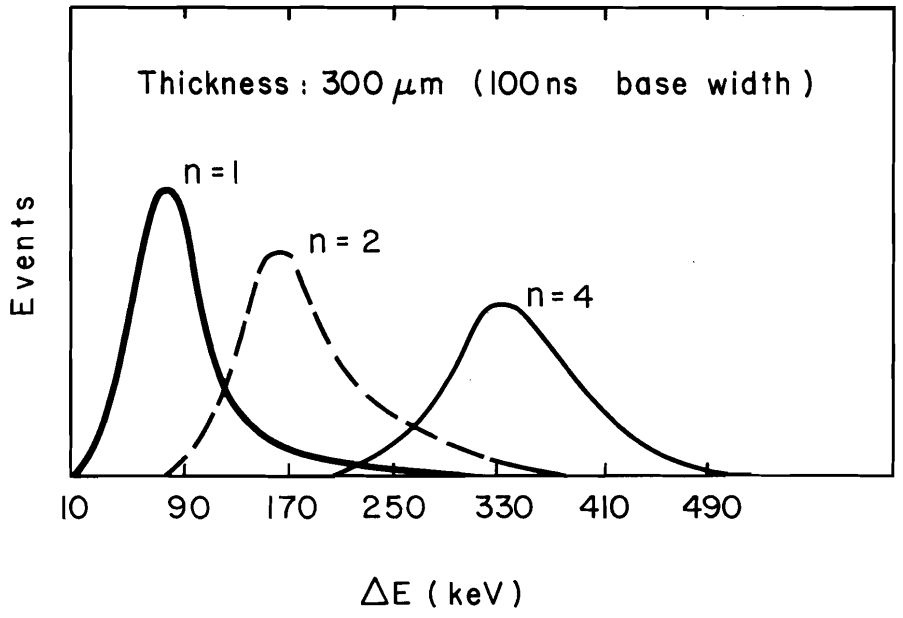

Fig. 7.- Pulse height distribution of a silicon layer for different number of crossing particles.

The pulse height pattern of the target allows to identify the production and the decay points of D-mesons as steps in the measured multiplicity. Two examples are shown in Fig. 8 for events which are identified in the spectrometer as good candidates for associate charmed meson production. The interaction point is signalled in general by a spike due to the coherent recoil of the silicon nucleus.

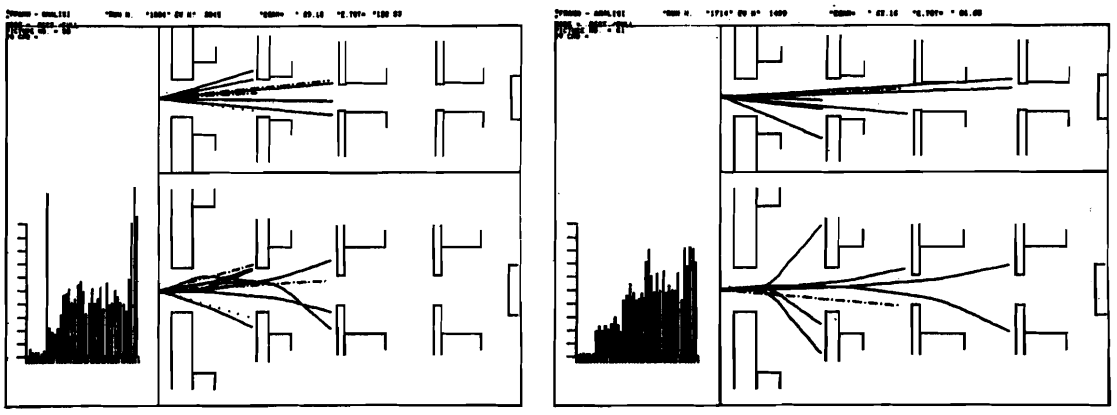

Fig. 8.- Two examples of pulse height pattern in the target. In the first event the coherent signal in the interaction layer is particularly evident. The final step has been disregarded since it extends over only 3 layers. The second event shows both decays in the target.

About 1.2 Million events have been examined selecting only final states with at least 6 charged particles in order to enhance the number of D^+D^- decays. Also events with odd number of prongs (7 or 9) have been accepted to allow for the loss of the pion from the D^* decay outside the acceptance of the spectrometer.

Since the target does not give any information on how particles must be associated to form a D - meson, particles have been subdivided into two groups with masses M_1 and M_2 and all combinations are examined in turn. A combination is considered only

i) if it contains a charged kaon candidate and,
ii) when the number of charged particles is odd, if it corresponds to a Cabibbo allowed $D^{\pm}$ decay channel.

The first loose selection applied to the data requires at least one group of particles to have a mass between 1.75 and 2.1 GeV, consistent with a D or a D^*. The distribution of the combinations is plotted against the variable M_1+M_2 in Fig. 9a. This plot gives a global view of the event and should show peaks corresponding to $D\bar{D}, D\bar{D}^*+D^*\bar{D}, D^*\bar{D}^*$ final states. The absence of any structure in the quoted mass region shows that the selection criteria are not stringent enough.

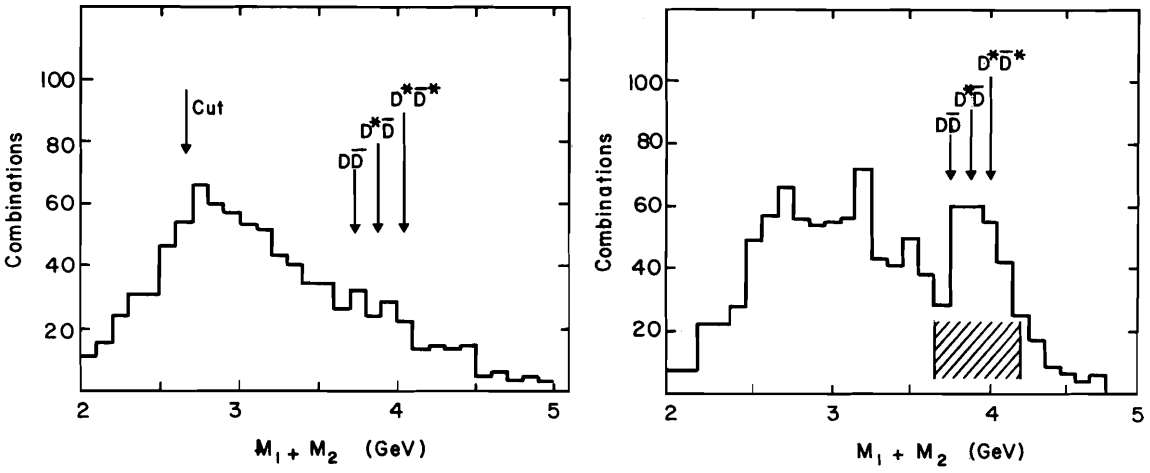

Fig. 9a).- Number of combinations vs. M_1+M_2 without any selection in the target
b) same plot after selection of events with step structure in the target.

All events are then examined in the target and only those which show a step structure are retained, a step being identified if it extends at least over four layers. Target patterns starting with a single spike in a layer, followed by a level of zero and by one or two steps, are ignored in this analysis since they correspond to the production and decay of $D^0(D^{0*})-\bar{D}^0(\bar{D}^{0*})$ states. The M_1+M_2 distribution for the remaining events, plotted in Fig. 9b, has now a clear structure in the region of charmed meson pairs. An inspection of the multiplicity components of this peak shows that charmed meson production becomes relatively more abundant as the multiplicity increases (see Fig. 10a, b).

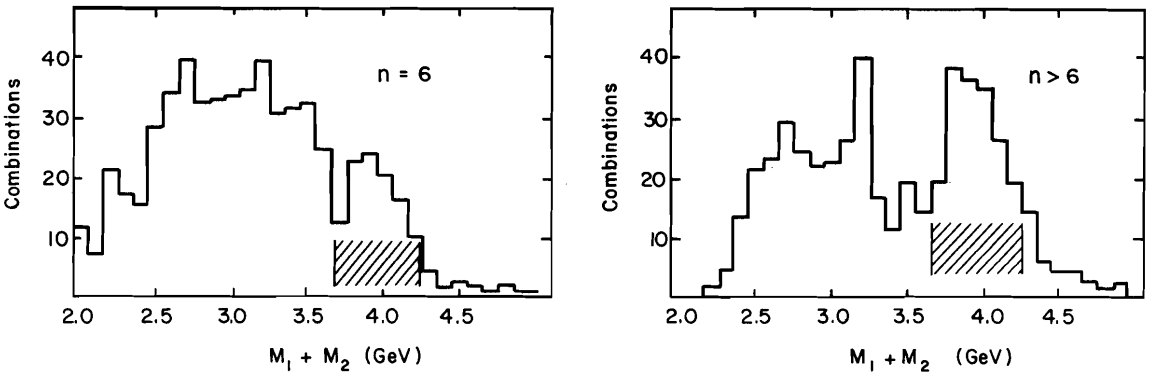

Fig. 10 a,b) M_1+M_2 distribution of selected events for different multiplicity samples.

A better evidence of the charmed nature of these events is given by the D-D^* peak shown in Fig. 11 by the distribution of M_2 measured for those combinations which have, on the other side, a value of M_1 in the D^* region ($1.9 < M_1 < 2.1$ GeV).

All events with a step structure in the target pattern and at least one combination falling in the mass interval $3.65 < M_1+M_2 < 4.2$ GeV are used to measure the lifetime of $D^{\pm}$ - mesons.

The sample consists of 63 events with a single step and of 12 events with two steps (24 decays). The distribution of the path length density, $dN/d\ell$, is plotted versus ℓ in Fig. 12, after correcting for the finite length of the target. A clear exponential fall is shown by the data, in contrast with the flat behaviour of the ℓ-distribution obtained for background steps due to γ-ray conversion and to pion interactions in the target itself.

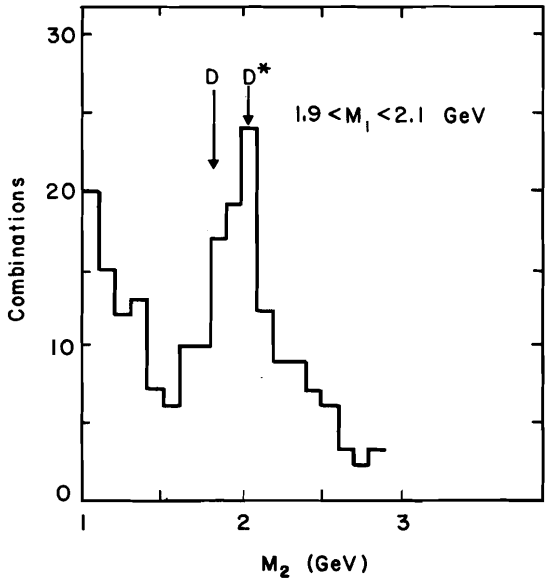

Fig. 11.- M_2 distribution when M_1 is fixed on the D^* mass.

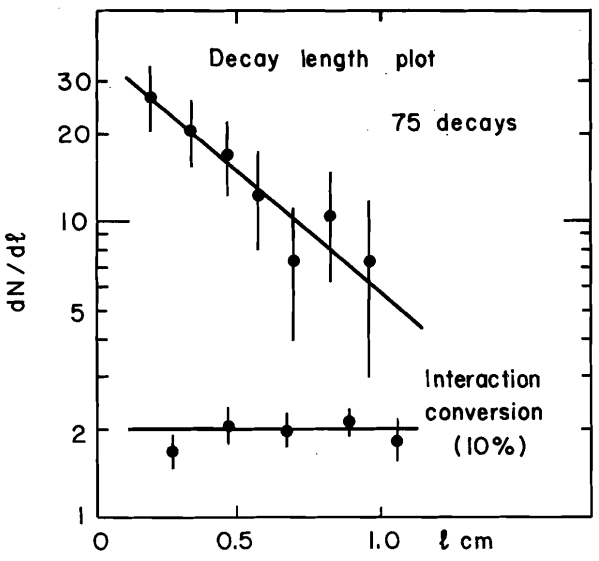

Fig. 12.- Distribution of decay paths for selected events a) and for background b).

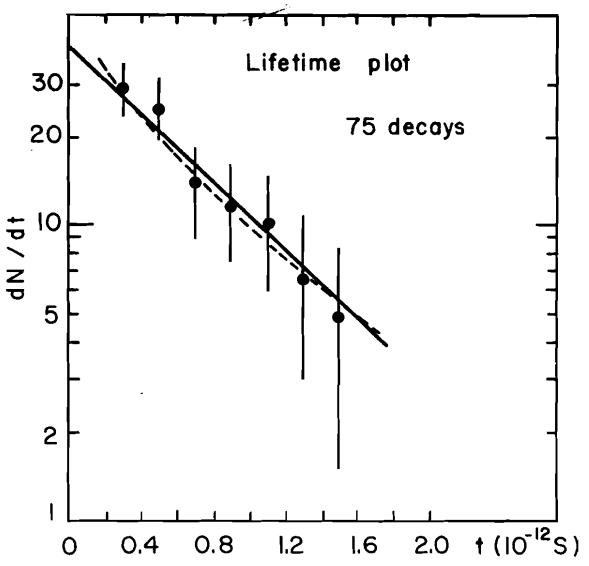

Fig. 13.- Distribution of decay times. The full line is a single slope fit to the data while dashed line contains 20% of D^0-decay with $\tau = 3 \cdot 10^{-13}$ s.

This distribution has been obtained by analyzing with the same procedure a sample of events falling outside the selected mass region. Most of the events characterized by fake steps are skipped during the analysis by identifying the electrons in the spectrometer or by requesting that no step show an overshoot at the beginning, typical of incoherent interactions. A few events, however, fulfill all selection criteria defined for decay steps and cannot be rejected in the analysis of the target pattern. The rate of these events amounts to 10% of the final sample of 75 steps. In the determination of the lifetime this background has been taken into account by skipping several times 7 events at random in ℓ and by averaging the resulting values of τ.

The determination of the decay time from the measurement of the decay path requires the knowledge of the energy of the D-mesons. In this preliminary analysis no effort has been done to identify in a unique way the decay channels of individual mesons since several combinations of the secondaries of an event can fall around the D-mass within a window of ±100 MeV. The energy of both mesons has then been defined as half the energy of the event. This approximation contributes negligibly to the error on the lifetime due to the small relative velocity of the D-mesons, the production of which is almost confined at threshold by the request of coherence on nuclei.

The time distribution obtained using all 75 decays is shown in Fig. 13. This sample is dominated by D^+, D^- decay but contains a contamination of D^0 decay mostly through $D^{*+} \to D^0 \pi^+$ decay. It has been evaluated, on the basis of known branching ratios, of the production mass spectrum and of spin and isospin conservation, that the contamination amounts to $\sim$ 20% if $\tau_{D^0} = 3 \cdot 10^{-13}$s and becomes smaller for shorter lifetimes.

A fit to the whole sample with a single slope, corrected for the 10% background described above, gives

$$\tau_{D^\pm} = (7.0^{+2.5}_{-1.6}) \times 10^{-13} \text{ s} \quad .$$

If the fit is limited to data measured at $t > 6.10^{-13}$ s, the D^0 contamination decreases to below 10% and the best fit value is

$$\tau_{D^\pm} = (8.1^{+5.5}_{-3.0}) \times 10^{-13} \text{ s} \quad .$$

In the same way, an overall fit to the data including 20% D^0 decays with $\tau_{D^0} = 3.10^{-13}$ s, gives

$$\tau_{D^\pm} = (8.0^{+2.5}_{-2.0}) \times 10^{-13} \text{ s} \quad .$$

This result is in good agreement with what determined by the Emulsion Spectrometer group [see Table 4] and by the bubble chamber experiments described above. Since the same agreement can be found among the corresponding results presented on τ_{D^0}, it is now fairly well established that τ_{D^0} is about 3 times shorter than $\tau_{D^\pm}$, in agreement with what deduced from the analysis of inclusive electron spectra at SPEAR [6].

REFERENCES

[1] M. Aguilar-Benitez et al., Charm Particle Production in 360 GeV π^-p and 360 GeV pp interactions,

[2] K. Abe et al., Photoproduction of charmed particles at 19.5 GeV, paper No.156; submitted to this Conference

[3] J. D. Prentice, Rapporteur's talk at International Conference on High Energy Physics, Lisbon 1981

[4] E. Albini et al., Preliminary results on an electronic measurement of $D^\pm$ lifetime, submitted to the International Conference on High Energy Physics, Lisbon 1981. Updated results of this analysis are presented in this talk.

[5] S.R. Amendolia et al., Nucl. Instr. and Meth. No. 176 (1980) 449. G. Bellini et al., Active target for lifetime measurements of charmed particles and related signal processing, submitted to Nucl. Instr. and Meth.

[6] W. Bacino et al., Phys. Rev. Lett. No. 45 (1980) 329.